Non – Linear Chemotactic Hydromagnetic Bioconvection

Prof. Dr. P. K. Srimani
R&D,Director (DSI)
Bangalore

Mrs. Radha.D
Assistant Professor, Dept of Mathematics,
BMS College of Engineering, Bangalore

Abstract

The effect of external magnetic field on the chemotactic bacterial bioconvection by considering a Continuum model is investigated. Chemotaxis causes cells to swim out of the plume because the high concentration of the cells constituting the plumes leads to a lower concentration of oxygen in the surrounding fluid. Further world's major portion consists of bio-mass; therefore it is of immense interest and at most importance to study bioconvection under different types of constraints. A similarity solution is found for the plume in which the cell flux and the volume flux could be matched to those in the boundary layer and also outside the suspension regions. Axisymmetric plumes is formed by applying two scales one with respect to the radial co-ordinate and the other with respect to the similarity variable. The effects of magnetic field are remarkable and encouraging and the computed results are in excellent agreement with those of hydrodynamic case in the limiting case.

1. Introduction

The spontaneous formation of patterns in suspensions of swimming microorganisms due to their tactic nature viz. oxytactic, gyrotactic, chemotactic etc., is termed as bioconvection. The microorganisms exhibiting bioconvection have the following key features: (i) They are denser than water (ii) They swim upwards due to their tactic nature. This leads to an unstable situation in the system and thus an overturning instability develops leading to pattern formation [1][2][3]. Also Magnetic field has a strong influence on the system in many real time situations. Experiments on bioconvection containing suspensions of bacteria (Bacillus Subtilis) have revealed the formation of Falling plumes (Figure 1.) when the system becomes unstable.

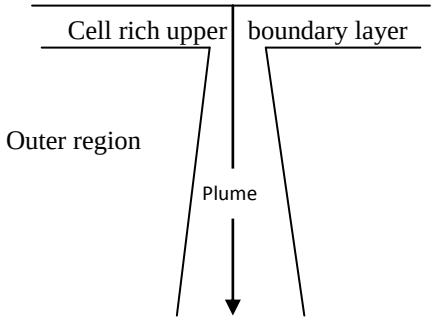

Figure 1. Formation of Bioconvection Plume

Some literatures pertaining to bioconvection in deep chambers are [4][5]. The study of such a phenomenon has a variety of applications in biological and physiological problems. Further, chemotaxis and oxygen consumption are important in setting up the basic state and soon after, the resulting plumes are entirely buoyancy driven and the cells are merely advected. In such cases, the velocity would vary across the plume [6][7] . The present work investigated the nonlinear Hydromagnetic bioconvection in order to study the effect of magnetic field on the formation of falling plumes (Axisymmetric) where the oxygen consumption and chemotaxis are important. The model constituted the quasi – steady situation in which an upper boundary layer containing a high concentration of bacteria feeds a falling plume of cell-rich fluid. The suspension was divided into three separate regions as shown in Figure 1, a cell-rich upper boundary layer of known thickness λ, a falling plume of unknown width ε which also contained a high concentration of bacteria and the fluid outside the plume which had to circulate in order to conserve mass. Here, the assumption of the axisymmetric nature of the plume reduced the 3D-problem to 2D-problem [8]. No much literature is available in this direction. The solutions were obtained by a Fast Computational Technique.

2. Mathematical Formulation

The bacterial suspension (Bacillus Subtilis) contained in a deep chamber reveal the development of a thin upper boundary layer of cell-rich saturated fluids which becomes unstable, leading to the formation of falling plumes which is a complex phenomenon. This was used as a basis for our mathematical model. The whole suspension was under the influence of uniform magnetic field .

The dimensionless governing equations are:

The equation of cell conservation

$$\frac{\partial N}{\partial t} = \nabla.\left[H(\theta)\nabla N - UN - H(\theta)\gamma N\nabla\theta\right] \quad (1)$$

The equation of oxygen concentration

$$\frac{\partial \theta}{\partial t} = \nabla.\left[\delta\nabla\theta - U\theta - H(\theta)\delta\beta N\right] \quad (2)$$

The Navier – Stokes equation (with Boussinesq approximation)

$$Sc^{-1}\left[\frac{\partial U}{\partial t} + (U.\nabla)U\right] = -\nabla P_e + \nabla^2 U + \Gamma N - B^*(H.\nabla)H \quad (3)$$

The conservation of mass

$$\nabla.U = 0 \quad (4)$$

The magnetic induction equation

$$\frac{\partial H}{\partial t} + (U.\nabla)H = (H.\nabla)U + P_m\nabla^2 H \quad (5)$$

The variables are non – dimensionalized as :

$$\nabla = \frac{1}{h}\nabla, N = \frac{\tilde{N}}{N_0}, \theta = \frac{\tilde{C} - C_{min}}{C_0 - C_{min}}, D_N = D_{N0}H(\theta),$$

$$V = bV_sH(\theta)\nabla\theta, K = K_0H(\theta).bV_s, t = \frac{TD_{N0}}{h^2},$$

$$U = \frac{\tilde{U}h}{D_{N0}}, H = \frac{\tilde{H}}{H_0}$$

Where h is the Depth of the chamber
V_s:It has dimensions of velocity
N_0 : Initial cell concentration
U : Saturated fluid velocity
D_{N0}, K_0:Constants
D_N : The cell diffusivity
θ : The oxygen concentration
C_0 :Initial Concentration
$H(\theta)$: The step function
T : The time
H_0 : The constant magnetic field

2.1 Dimensionless Parameters

$$\beta = \frac{K_0N_0h^2}{D_c(C_0 - C_{min})}, \gamma = \frac{bV_s}{D_{N0}}, \delta = \frac{D_c}{D_{N0}}, B^* = \frac{\mu^*H_0^2h^2}{\rho_w\nu D_{N0}}$$

$$\Gamma = \frac{\upsilon N_0gh^3(\rho_c - \rho_w)}{\nu D_{N0}\rho_w}, Sc = \frac{\nu}{D_{N0}}, P_m = \frac{\nu_m}{D_{N0}}$$

β : Strength of Oxygen consumption relative to its diffusion
γ : Measures the relative strengths of directional and random swimming
δ : Ratio of Oxygen diffusivity to cell diffusivity
Γ : Bio-Rayleigh number
Sc : Schmidth number
P_m : Magnetic Prandtl number
ν : Kinematic viscosity of the fluid
ρ_c, ρ_w : Densities of cell and water
g : Acceleration due to gravity
ν : Volume of a cell
B^* : Modified Hotmann number
μ^* : MagneticPreamibility
ν_m : Magnetic viscosity of the fluid

2.2 Boundary Conditions

i. No slip condition at Z = 1(bottom of the chamber).
ii. Stress free condition at the upper surface of the chamber, i.e., at Z = 0.
iii. The vertical components of velocity vanish at both the boundaries.
iv. Zero cell – flux at both the boundaries.
v. Zero oxygen flux at the bottom surface and C = C_o at the free surface.
vi. H = 0 at both the boundaries
vii. The vertical components of velocity vanish at both the boundaries.

Mathematically,

At Z = 0,

$$U.\hat{Z} = 0, \frac{\partial^2}{\partial Z^2}\left[U.\hat{Z}\right] = 0, \theta = 1$$

$$H(\theta)\frac{\partial N}{\partial Z} - \gamma NH(\theta)\frac{\partial \theta}{\partial Z} = 0, \left[H\hat{Z}\right] = 0.$$

At Z = 1,

$$U.\hat{Z} = 0, U\times\hat{Z} = 0, \frac{\partial\theta}{\partial Z} = 0, \frac{\partial N}{\partial Z} = 0, H.\hat{Z} = 0$$

3. Axisymmetric Plumes using Radial Co-ordinates

In the plume, the radial co-ordinate is scaled as

$$R = \varepsilon r, O < \varepsilon << 1 \quad (6)$$

Rescaling:

$$N = N_An, \theta = 1 + C_AC, W = W_Aw,$$
$$U = \varepsilon W_Au, P = P_AP \quad (7)$$

where N_A , C_A, W_A , and P_A are scale factors. Then the axisymmetric governing equations (Neglecting O (ε^2) terms) are,

$$\frac{1}{r}\frac{\partial n}{\partial R}+\frac{\partial^2 n}{\partial r^2}=\varepsilon^2 W_A\left[u\frac{\partial n}{\partial r}+w\frac{\partial n}{\partial z}\right]+\gamma C_A\left[\frac{\partial n}{\partial r}\frac{\partial C}{\partial r}+\frac{n}{r}\frac{\partial C}{\partial r}+n\frac{\partial^2 C}{\partial r^2}\right] \quad (8)$$

$$\frac{\varepsilon^2 W_A}{\delta}\left[u\frac{\partial C}{\partial r}+w\frac{\partial C}{\partial Z}\right]+\frac{\varepsilon^2\beta N_A n}{C_A}=\frac{\partial^2 C}{\partial r^2}+\frac{1}{r}\frac{\partial C}{\partial r} \quad (9)$$

$$\frac{u}{r}+\frac{\partial u}{\partial r}+\frac{\partial w}{\partial Z}=0 \quad (10)$$

$$\varepsilon^2 W_A Sc^{-1}\left[u\frac{\partial u}{\partial r}+w\frac{\partial u}{\partial Z}\right]=\frac{-P_A}{W_A}\frac{\partial p}{\partial r}+\frac{\partial^2 u}{\partial r^2}+\frac{1}{r}\frac{\partial u}{\partial r}-\varepsilon^2 B^*\frac{H_A^{\,2}}{W_A}\left[h_X\frac{\partial h_X}{\partial r}+h_Z\frac{\partial h_X}{\partial Z}\right] \quad (11)$$

$$\varepsilon^2 W_A Sc^{-1}\left[u\frac{\partial w}{\partial r}+w\frac{\partial w}{\partial Z}\right]=-\varepsilon^2\frac{P_A}{W_A}\frac{\partial p}{\partial Z}+\varepsilon^2\frac{N_A}{W_A}\Gamma n+\frac{\partial^2 w}{\partial r^2}+\frac{1}{r}\frac{\partial w}{\partial r}-B^*\varepsilon^2\frac{H_A^{\,2}}{W_A}\left[h_X\frac{\partial h_Z}{\partial r}+h_Z\frac{\partial h_Z}{\partial Z}\right] \quad (12)$$

$$\varepsilon^2 W_A\left[u\frac{\partial u}{\partial r}+w\frac{\partial u}{\partial Z}\right]=\varepsilon^2 H_A\left[h_X\frac{\partial u}{\partial r}+h_Z\frac{\partial u}{\partial Z}\right]+P_m\frac{H_A}{W_A}\left[\frac{1}{r}\frac{\partial h_X}{\partial r}+\frac{\partial^2 h_X}{\partial r^2}\right] \quad (13)$$

$$\varepsilon^2 W_A\left[u\frac{\partial w}{\partial r}+w\frac{\partial w}{\partial Z}\right]=\varepsilon^2 H_A\left[h_X\frac{\partial w}{\partial r}+h_Z\frac{\partial w}{\partial Z}\right]+P_m\frac{H_A}{W_A}\left[\frac{1}{r}\frac{\partial h_Z}{\partial r}+\frac{\partial^2 h_Z}{\partial r^2}\right] \quad (14)$$

Here,

$W_A=\varepsilon^{-2}$ (to retain advection terms)
$C_A=2/\gamma$ (to retain chemotaxis term)
$N_A=\lambda/\varepsilon^2$ (to retain the oxygen consumption term in 9)
Γ = O ($\lambda^{-1}\varepsilon^{-2}$) (to retain the buoyancy term in 12)
$P_A=\varepsilon^{-4}$ (to retain the pressure term in 12)
$H_A=\varepsilon^{-2}$ (to retain the induction term in 14)

This leads to $\frac{\partial p}{\partial r}=0$ hence p = p (Z) in (11). (15)

Substituting for C_A, W_A and N_A in (8) and (9) :

$$u\frac{\partial n}{\partial r}+w\frac{\partial n}{\partial Z}+2\frac{\partial n}{\partial r}\frac{\partial C}{\partial r}+2\frac{n}{r}\frac{\partial C}{\partial r}+2n\frac{\partial^2 C}{\partial r^2}-\frac{1}{r}\frac{\partial n}{\partial r}-\frac{\partial^2 n}{\partial r^2}=0 \quad (16)$$

$$\frac{1}{\delta}\left[u\frac{\partial C}{\partial r}+w\frac{\partial C}{\partial Z}\right]+n\left[\frac{1}{r}\frac{\partial C}{\partial r}+\frac{\partial^2 C}{\partial r^2}\right]=0 \quad (17)$$

Differentiating (12) w.r.t. r and substituting for $N_A W_A$, H_A and Γ :

$$Sc^{-1}\left[\frac{\partial u}{\partial r}\frac{\partial w}{\partial r}+u\frac{\partial^2 w}{\partial r^2}+\frac{\partial w}{\partial r}\frac{\partial w}{\partial Z}+w\frac{\partial^2 w}{\partial r\partial Z}\right]=\tilde{\Gamma}\frac{\partial n}{\partial r}+\frac{\partial^3 w}{\partial r^3}+\frac{1}{r}\frac{\partial^2 w}{\partial r^2}-\frac{1}{r^2}\frac{\partial w}{\partial r}-B^*\left[\frac{\partial h_X}{\partial r}\frac{\partial h_Z}{\partial r}+h_Z\frac{\partial^2 h_Z}{\partial r^2}+\frac{\partial h_Z}{\partial r}\frac{\partial h_Z}{\partial Z}+h_Z\frac{\partial^2 h_Z}{\partial r\partial Z}\right] \quad (18)$$

Differentiating (14) w.r.t r and substituting for H_A,W_A

$$\left[\frac{\partial u}{\partial r}\frac{\partial w}{\partial r}+u\frac{\partial^2 w}{\partial r^2}+\frac{\partial w}{\partial r}\frac{\partial w}{\partial Z}+w\frac{\partial^2 w}{\partial r\partial Z}\right]=\left[\frac{\partial h_X}{\partial r}\frac{\partial w}{\partial r}+h_X\frac{\partial^2 w}{\partial r^2}+\frac{\partial h_Z}{\partial r}\frac{\partial w}{\partial Z}+h_Z\frac{\partial^2 w}{\partial r\partial Z}\right]+P_m\left[\frac{-1}{r^2}\frac{\partial h_Z}{\partial r}+\frac{1}{r}\frac{\partial^2 h_Z}{\partial r^2}+\frac{\partial^3 h_Z}{\partial r^3}\right] \quad (19)$$

Now, imposing the boundary conditions:

$$\frac{\partial n}{\partial r}=0,\frac{\partial C}{\partial r}=0,u=0,\frac{\partial w}{\partial r}=0$$

$$Also, r\to\infty, n\to 0,\frac{\partial C}{\partial r}\to 0, w\to 0$$

3.1 Similarity solution for axisymmetric case

In order to obtain a similarity solution [9][10] for (16), (17), (18), (19) the solution was posed of the form

$$h::Z^a, w::Z^b, n::Z^c, C::Z^d, u::Z^{a+b+1} \quad (20)$$

(h: width of the plume, a = ½, b = 0, c = -1, d = 0) Since h :: $Z^{1/2}$, the similarity variable is defined as

$$\eta=\frac{r}{Z^{1/2}} \quad (21)$$

Assuming the solution in the form

$$n=Z^{-1}H(\eta), C=G(\eta), \psi=ZF(\eta), u=Z^{\frac{-1}{2}}\left(\frac{F}{\eta}-\frac{F'}{2}\right), w=\frac{-F'}{\eta} \quad (22)$$

(ψ : Stream functions, Primes denote differentiation w.r.t η). Substituting these into (16) and integrating once w.r.t η with the boundary conditions at η = 0, we get the following: $HF+2\eta HG'-\eta H'=0$ (23)

Substituting into (17)

$$\eta G''+G'-\frac{1}{\delta}G'F-\eta H=0 \quad (24)$$

Substituting into (18)

$$\frac{1}{\eta}F'''-\frac{1}{\eta^2}F''+\frac{1}{\eta^3}F'+Sc^{-1}\left[\frac{1}{\eta^3}FF'-\frac{1}{\eta^2}FF''\right]-\tilde{\Gamma}H-B^*\left(\frac{1}{\eta^3}MM'-\frac{1}{\eta^2}MM''\right)=0 \quad (25)$$

Substituting into (19)

$$M = F \qquad (26)$$

The boundary conditions are ,

At $\eta = 0$:

$$H' = G' = \frac{F}{\eta} - \frac{F'}{2} = \frac{F'}{\eta^2} - \frac{F''}{\eta} = 0$$

At $\eta \to \infty$:

$$H \to 0, G' \to 0, \frac{F'}{\eta} \to 0, \frac{M'}{\eta} \to 0$$

4. Solution

For $\gamma \neq 0$, CFD technique is employed. However for $\gamma = 0$ (i.e., when the chemotaxis is unimportant in the plume) analytical solutions are possible with β = O (1), $C_o = 1$, $N_o = \varepsilon^{-2}$ and $\Gamma = \varepsilon^{-2}\tilde{\Gamma}$. Following [4] [8] the solutions for the equations (23, 24, 25, 26) are found to be (see table 1)

$$B = \frac{-12}{1 + Sc^{-1} - B^*}$$

$$C = \left(\frac{192A^2}{1 + Sc^{-1} - B^*} \right) \frac{1}{\tilde{\Gamma}}$$

Table 1. Solutions for F, H, G'

At Sc=1, δ=1	At Sc=2, δ=1
$F = \frac{-12A\eta^2}{(2-B^*)(1+A\eta^2)}$	$F = \frac{-24A\eta^2}{(3-2B^*)(1+A\eta^2)}$
$H = \frac{192A^2}{\tilde{\Gamma}(2-B^*)(1+A\eta^2)^{\frac{6}{2-B^*}}}$	$H = \frac{384A^2}{\tilde{\Gamma}(3-2B^*)(1+A\eta^2)^{\frac{12}{3-2B^*}}}$
$G' = \frac{96A^2\eta}{\tilde{\Gamma}(2-B^*)(1+A\eta^2)^{\frac{6}{2-B^*}}}$	$G' = \frac{192A^2\eta}{\tilde{\Gamma}(3-2B^*)(1+A\eta^2)^{\frac{12}{3-2B^*}}}$

Also solutions satisfy the boundary conditions at $\eta = 0$ and $\eta \to \infty$.

$$A^2 = \frac{Q\tilde{\Gamma}(2-B^*)(8-B^*)}{2304} \quad for\ Sc = 1$$

$$A^2 = \frac{Q\tilde{\Gamma}(3-2B^*)(15-2B^*)}{9216} \quad for\ Sc = 2$$

Since $\left[\int_0^\infty HF'd\eta = -Q \right]$

5. Results and Discussion

In this study, the deep chamber experiments of Figure.1 have been modelled in three separate regions:

a. an upper boundary layer of depth λ_R
b. a falling plume of width ε
c. the region outside the plume.

In the sections 3 and 4, solutions for the cell and the oxygen concentration and the fluid velocity in the upper boundary layer are determined under the influence of a uniform vertical magnetic field. The solutions are found to depend on the parameters like, Sc (Schmidth number), Q (the cell flux), $\tilde{\Gamma}$ (Bio-Rayleigh number), B^* (Magnetic Parameter) and δ (diffusivity ratio). The computations are performed using the MATLAB tool; the computed results are presented through graphs in Figures 2 to 14.

The following observations are made: In Figures 2,3,4,5. the effect of variation in the magnetic parameter B^* on the profiles of velocity $w\left(=-F^1/\eta\right)$, the cell concentration H and the oxygen concentration G is studied for the values, Sc = δ = $\tilde{\Gamma}$ = Q = 1.0. Here, the oxygen concentration is considered as $\theta = \left(1 + \left(2/\gamma\right) G(\eta)\right)$ where γ is assumed to be always positive so that, all the bacteria are active. In Figure.2 the effect of similarity variable η on the F profile are shown. F decreases enormously and remains constant as $\eta \to \infty$ for all values of B^*. Further, F is negative and its value is highest in the hydrodynamic case. In other words, F increases in absolute value as B^* increases, and the vertical fluid velocity w, at the center of the plume increases indicating that the horizontal fluid flow into the plume increases. From Figure.5, w→0 as $\eta \to \infty$ as expected. In Figure.3 the effect of similarity variable on H profile is shown, it reveals that, as B^* decreases the cell concentration in the plume increases as expected. Physically it means that, the higher the concentration of the cells, the greater is the consumption of oxygen which means that the oxygen concentration at the center of the plume decreases. In Figure.4 the effect of similarity variable on G' profile is shown. Clearly the width of the plume decreases as B^* increases. The oxygen concentration is more in the hydrodynamic case (B^* = 0) when compared to the hydro magnetic case ($B^* \neq 0$).

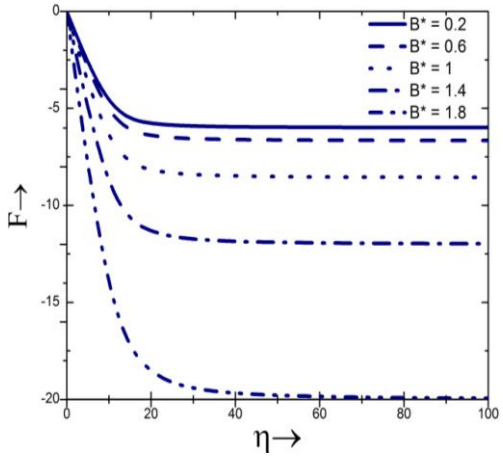

Figure 2. F vs η

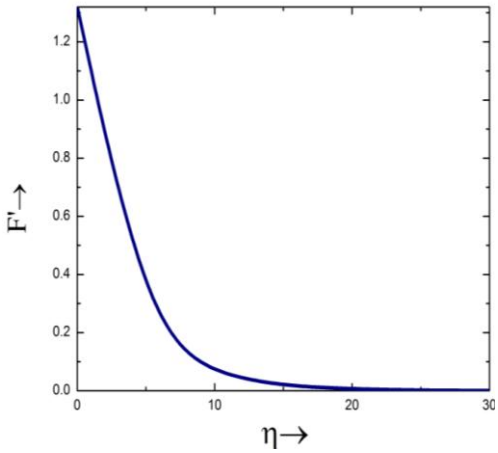

Figure 5. F′ vs η

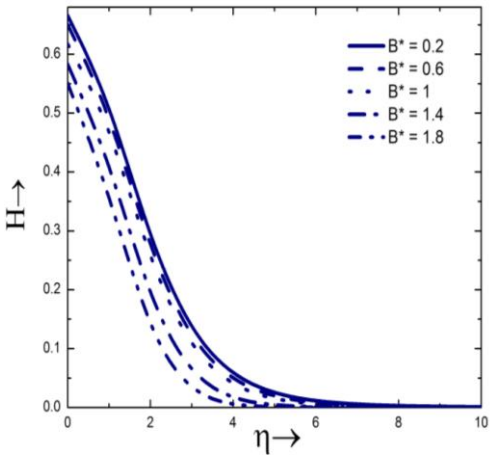

Figure 3. H vs η

Figures 6,7, 8. reveal the effect of variation of Q (= 0.5, 3, 5) on the profiles of F, H, G'. As the cell flux increases, F slightly decreases and increases in absolute value. The values of F are considerably very large inside the plume and drastically decrease and become constant for large values of η and accordingly w→0 for large η .

Fig.7 reveals that the width of the plume drastically increases as the value of Q decreases and the plume becomes narrower for large values of Q. Thus, the high concentration of the cells leads to a greater consumption of oxygen which in turn reduces the oxygen concentration at the center of the plume. Thus, as the cell flux Q increases, the vertical fluid velocity w, at the center of the plume increases and the values of M increases, indicating the increase in the horizontal fluid flow into the plume.

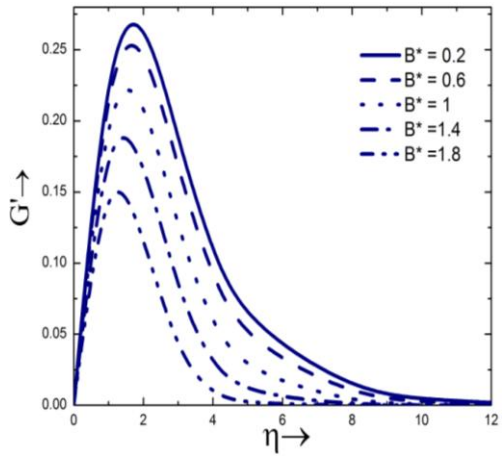

Figure 4. G′ vs η

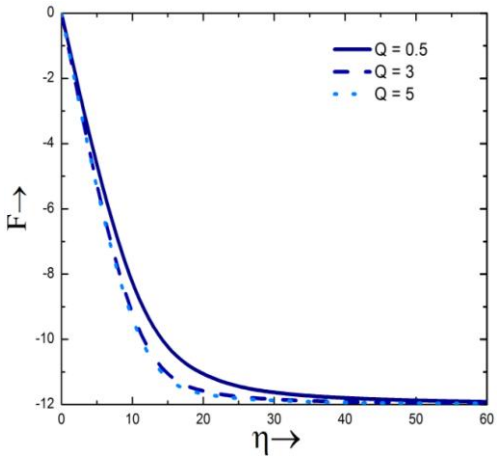

Figure 6. F vs η

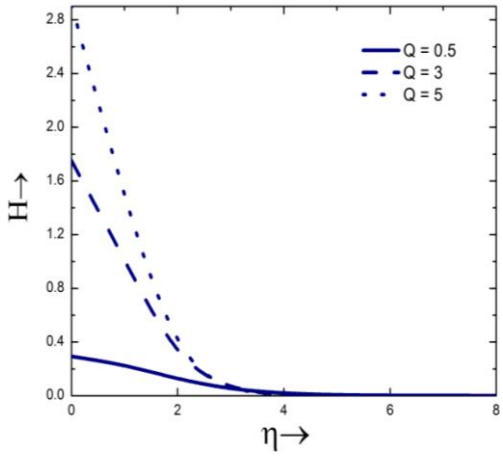

Figure 7. H vs η

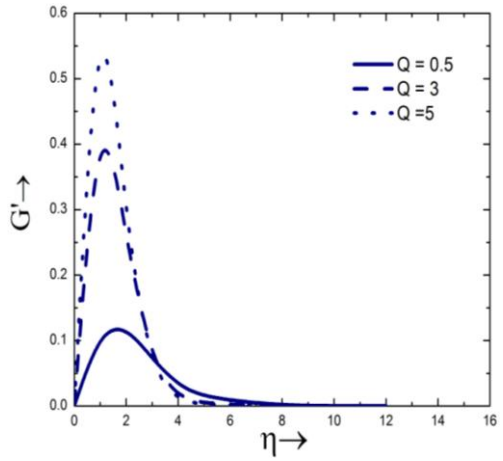

Figure 8. G′ vs η

From Figure 8., it is found that the oxygen concentration in the plume is high for large Q(= 5) and the width of the plume drastically increases as Q decreases. This clearly indicates that the oxygen concentration at the center of the plume is less since there is a greater consumption of oxygen in the plume for large Q.

Figures 9,10,11. represent the effect of variation of $\tilde{\Gamma}$ on the profiles F, H, G' for fixed values of the parameters $\left(Sc = \delta = B^* = 1\right)$. The values of $\tilde{\Gamma}$ considered are 0.2, 2 and 5.

The effect of buoyancy becomes important when $\tilde{\Gamma}$ is large. The cell concentration is more for small values of $\tilde{\Gamma}$ and the plume becomes narrower for large $\tilde{\Gamma}$. When the cell concentration in the centre of the plume increases, the plume becomes narrower, accordingly the oxygen profile becomes narrower and the oxygen concentration at the center of the plume increases. The consumption of oxygen will be more. Therefore, the velocity of the fluid in the center of the plume will be larger when the buoyancy force is dominant. But w→0 more rapidly than for small values of $\tilde{\Gamma}$. The decrease in M for the increase in $\tilde{\Gamma}$ indicates that less fluid is entrained by the plume.

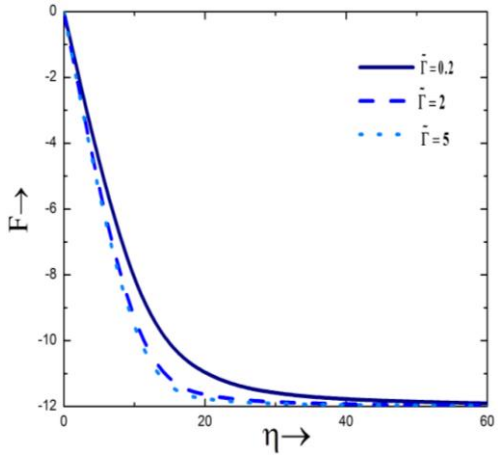

Figure 9. F vs η

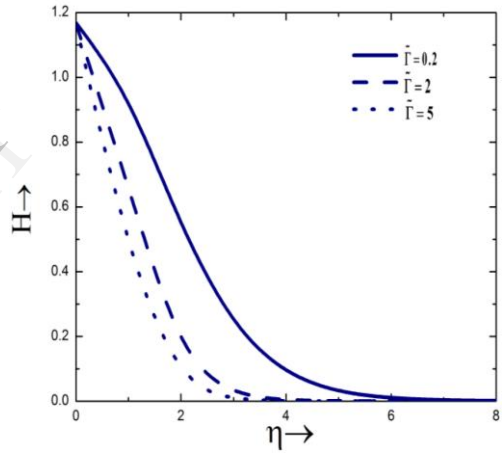

Figure 10. H vs η

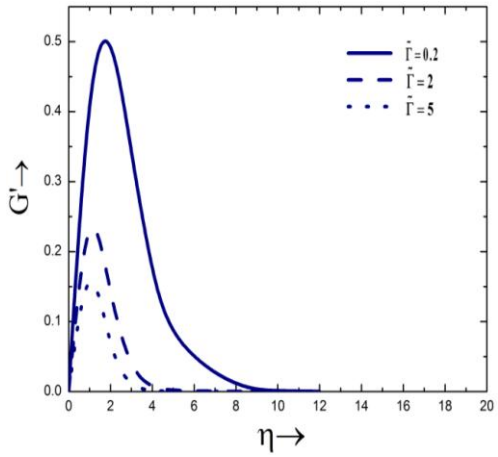

Figure 11. G′ vs η

Figures 12,13,14. present the graph of the profiles F, H, G' when the values of Sc (= 1, 2) are varied. The other parameters have fixed values viz., δ = 1, Q = 1 B^* = 1. It is observed that as in the hydrodynamic case (B^* = 0), the variation in Sc has a significant effect on the behaviour of the profiles. There is a drastic change in the values of F for Sc = 1 and 2. As Sc increased, F decreases rapidly and F→ a constant value as $\eta \to \infty$ as expected. The cell concentration will be more for Sc = 2 and accordingly the oxygen consumption in the plume will be more and there will be a reduction in the oxygen concentration in the plume.

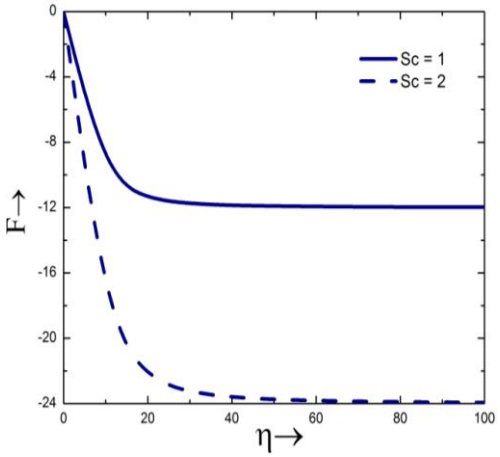

Figure 12. F vs η

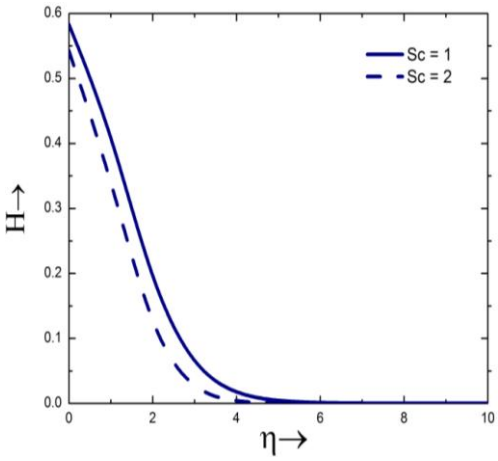

Figure 13. H vs η

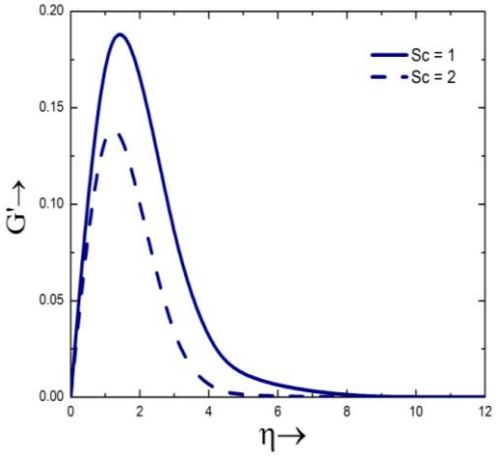

Figure 14. G′ vs η

Finally, it is concluded that (i) the governing dimensionless parameters have a remarkable effect in the hydrodynamic as well as in the hydromagnetic cases (ii) the qualitative nature of the profiles is almost the same in both the cases but there is a drastic difference in the quantitative nature of the profiles. Figure 1. clearly indicates the strong influence of the magnetic parameter on the present bioconvective system, these clearly suggest that the plume convection could be suppressed or enhanced through the proper choice of the magnetic parameter. The results are in excellent agreement with the hydrodynamic case.

References

[1] J.O.Kessler, Cooperative and concentrative phenomena of swimming microorganisms,Contemp.Phys.26, 1985 147 – 166.

[2] A.V.Kuznetsov, A.A. Avramenko, and P. Geng, A similarity solution for a falling plume in bioconvection of oxytactic bacteria in a porous medium, Int Commun Heat Mass Transfer,30,2003, 37 - 46

[3] T.J.Pedley, N.A.Hill, and J.O. Kessler, The growth of bioconvection patterns in a uniform suspension of gyrotactic micro–organisms, J.Fluid Mech, 195,1988, 223 – 238.

[4] A.J. Hillesdon, T.J. Pedley, and J.O. Kessler, The development of concentration gradient in a suspension of chemotactic bacteria, Bull. Math. Biol, 57: 2,1995, 99-344

[5] A.J. Hillesdon, and T.J. Pedley, Bioconvection in suspensions of oxytactic bacteria: linear theory, J. F.M, 1996, 324: 223 – 259.

[6] A.M. Metcalfe, et al., Bacterial bioconvection: weakly nonlinear theory for pattern selection, J. Fluid Mech, 1998, 370:249 – 270.

[7] S. Ghorai, and N.A. Hill, Gyrotactic Bioconvection in Three dimensions, Phys. Fluid, 2007, 19: 054107.

[8] S. Ghorai, and N.A. Hill, Gyrotactic Bioconvection in Three dimensions, Phys. Fluid, 2007, 19: 054107.

[9] C.S. Yih, Free convection due to a point source of heat, In Proc. 1st US Nat. Cong. Appl. Mech, (ed. E. Sternberg), 1951, pp. 941 – 947.

[10] A.M. Metcalfe, T.J. Pedley, Falling plumes in bacterial bioconvection,J. Fluid Mech. 445, 2001, 121 - 149.